THERMAL ANALYSIS AND MICROSTRUCTURAL STUDY OF POROUS β-TiNb INCORPORATED WITH TiH_2 POWDER VIA LOW-COST PROCESSING ROUTE

S. M. Hosnie[1], M. Yahaya[2], N.A. Haris[3] and M. H. Ismail[1]

[1]Centre for Advanced Materials Research (CAMAR), Faculty of Mechanical Engineering, Universiti Teknologi MARA, 40450 Shah Alam, Selangor, Malaysia.

[2]Mechanical Engineering Department, Politeknik Nilai, Kompleks Pendidikan Bandar Enstek, 71760 Bandar Enstek, Negeri Sembilan.

[3]Faculty of Mechanical Engineering, Universiti Teknologi MARA Campus Pasir Gudang, 81750, Masai, Johor, Malaysia.

Corresponding Author's Email: [1]hussain305@salam.uitm.edu.my

Article History: Received 29 September 2017; Revised 27 July 2018; Accepted 12 October 2018

ABSTRACT: In the development of Ti-based alloy bio-implant material, Titanium Hydride (TiH_2) which is commonly used as a pore former agent has become one of the new approaches of starting material via powder metallurgy processing route with the aim of low-cost production in the fabrication of Beta-typed Titanium Niobium (β-TiNb) alloy. However, the thermal behaviour of TiNb alloy by TiH_2 substitution is still not well understood. Thus, in the present work the compacted of Ti and Nb mixture was subjected to thermal analysis via differential thermal analysis (DTA) and dilatometry to evaluate thermal events existed during sintering process. It was found that the overall reaction had undergone four-step processes; the first two steps were subjected to the dehydrogenation process whereas the last two steps corresponded to the formation of TiNb alloy. In addition, the β phase of TiNb exhibited better appearance at 1200°C sintered temperature which was supported by X-ray Diffraction (XRD) analysis.

KEYWORDS: *TiNb Alloy; Titanium Hydride; Thermal Analysis; Dehydrogenation; Sintering Behaviour*

1.0 INTRODUCTION

Fabrication of new implant material based on Ti alloy has attracted much attention in biomedical research for hard tissue replacement such as hip and knee. The tremendous application of Ti alloy is due to excellent mechanical properties, corrosion resistance and good biocompatibility in the human body [1-2]. Nevertheless, certain Ti-based alloys exhibit high Young's modulus; for instance, Ti-6Al-4V (110 GPa) that is greater than human cortical bone which is in the range of 10 to 30 GPa [3]. As a consequence, the mismatch problem arises between bones and implant material leading to stress shielding to human bones [4]. Among all the Ti alloys that already exist, TiNb alloy has received a great interest. Due to promising biocompatible and low Young's modulus value (1.5~3 GPa) as reported in the literature [5], it is technically similar with human cancellous bone (~3 GPa) [6]. The low value of Young's modulus is owing to the porous structure and the formation of β-phase in the structure. On top of that, the Ti-40Nb is selected in the composition in accordance to the work patented by Davidson and Kovacs [7] which stated that Nb content between 35-50 by mass fraction has demonstrated low Young's modulus.

The utilization of Ti with other powders (as-mixed) as a starting material for Ti alloy formation is basically unfavourable because of the high cost of the raw material, problems of intermetallic phases and difficulties in machining [8]. The processing route needs a high vacuum to reduce the oxidation problem because Ti has a very high affinity for oxygen. Handling in a high vacuum may lead to the cost increase in production. Despite the high cost of Ti powder, a new approach to reduce the cost of production has been developed by incorporating TiH_2 powder instead of Ti powder [6, 9–11]. The usage of TiH_2 not only generates evenly distributed small pore , but it is also able to reduce the oxidation that subsequently prevents the intermetallic phases formation in the NiTi alloy case [6,12]. During the sintering process, the TiH_2 will undergo dehydrogenation process where H atom is released and eventually produces fresh generated Ti atom at approximately above 300˚C that is basically ready for an alloy formation. Below the 300˚C, the Ti particles are being protected from being oxidised as the Ti is bonded with H atoms [13].

The TiNb alloy has been successfully produced through two techniques namely arc melting [14] and powder metallurgy (PM) [5]. Each has specific advantages and limitations. With the concern towards intricate shape and geometry of implant components, PM is the promising processing candidate because it has the capability to produce the net final shape that minimizes or in some cases omits the secondary processes such as machining and drilling. Besides, through PM route, it is possible to obtain various pore sizes and mechanical properties by controlling the compacting and sintering condition [6].

There are limited studies regarding fabrication route because the fabrication of TiNb alloy incorporated with TiH_2 is a new approach. Due to limited study in the formation of TiNb that is fabricated using TiH_2 powder, the phase transformation during sintering is still not well understood. Hence, this study attempted to use thermal analysis method with the purpose to understand the sintering mechanism of TiNb alloy particularly on phase transformation to facilitate some insights on sintering profile for experimental work. By referring to thermal analysis result, the present study attempted in prolonging the reaction time at a certain temperature in order to fabricate Ti40Nb alloy with β-rich phase as well as high porosity. The present study employed a low-cost processing route by PM incorporated with TiH_2 powder that is expected to produce a new promising Ti-40Nb alloy for implanting material and to establish an alternative PM route which is economically sound.

2.0 EXPERIMENTAL

The mixed powder of TiH_2-40Nb (weight %) was attained from mixing TiH_2 powder (average particle size of 53 µm) and Nb powder (average particle size of 130 µm) to a composition of 40% Nb and 60% TiH_2, respectively. The powders were milled for 5 hours within 15 minutes interval with 12 repetitions at 200 rpm using a planetary ball mill, Retsch PM 400 model. Then, the mixed powder was consolidated at room temperature to form a green compact with a die cylindrical of 25 mm in size using a uni-axially die-compaction with a compact force of 9.81 kN. The green compact was subsequently cut into a rectangular shape with a dimension of 4 x 6 x 14 mm^3 in size for dilatometer analysis purpose. The cutting process was performed using a precision diamond cutter.

The thermal analysis of DTA was carried out under inert nitrogen gas atmosphere. The analysis of DTA was carried out by Linseis DTA L81 at the heating rate of 10°C/min with flow gas at the rate of 10 ml/min. The as-mixed powder sample with an initial weight of 49 ± 0.1 mg was inserted in alumina (Al_2O_3) crucible and heated up to 1200°C. Meanwhile, in order to investigate the shrinkage of the sample during the sintering process, the green compact was subjected to dilatometry analysis. Linseis Dilatometer L_{75} conducted the dilatometry measurements on a vertical configuration. The heating rate was kept constant as the DTA value was at 10˚C/min to have a similar parameter for the sintering process.

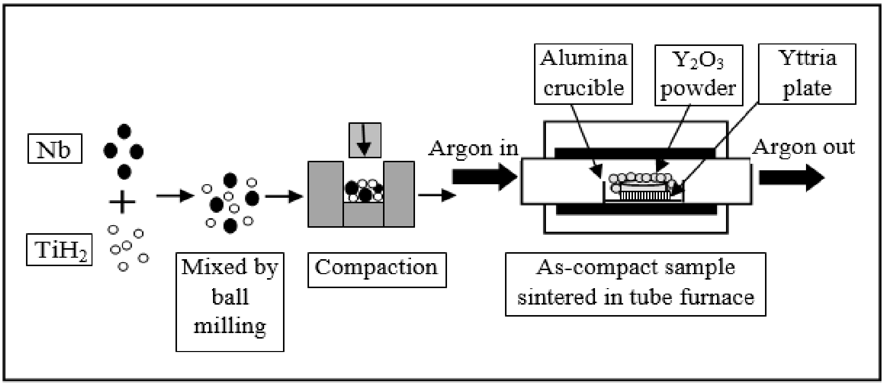

Figure 1: Schematic diagram of PM processing route under argon environment

The green compact was then sintered in a tube furnace with a heating rate of 5°C/min under an argon gas environment. A few steps had been carried out to reduce the oxygen uptake by the sample because the sintering did not occur in a vacuum condition. The Ti-Nb powder compact was firstly placed on yttria plate prior to being embedded with yttria (Y_2O_3). The yttria plate was placed on the alumina crucible so that the surface of the green compact was not in contact with alumina crucible. The sample on the yttria plate and one embedded by the yttria powder was not being oxidized as would have happened if only alumina crucible was used. The sintering was conducted at a sintering temperature of 1200°C. At the thermal event which was found after analyzing the thermal results, the reaction time was prolonged for 2 hours at the certain thermal event.

The phases changed from the raw powder, mixed powder to the as-sintered sample using X-ray diffraction analysis (XRD) where the XRD was performed using a Rigaku 3014, Japan. Phases in the present work were identified by matching their characteristic pattern peaks with those in the files of the Joint Committee on Powder Diffraction Standards (JCPDS).

3.0 RESULTS AND DISCUSSION

3.1 Differential Thermal Analysis (DTA)

Figure 2 shows the DTA result of the powder mixture of TiH_2-40Nb, indicating the change in the heat flow with respect to the temperature. According to this curve, the reaction in the formation of TiNb alloy can be divided into four main steps whereby the first two stages represented the dehydrogenation process while the other two stages represented the formation reaction of TiNb alloy. In accordance with literature [16–18], the dehydrogenation process of TiH_2 undergoes a two-step reaction which can be expressed as

$$TiH_2 = TiH_x + H_2 (x = 0.7 \approx 1) \qquad (1)$$

$$TiH_2 = \alpha(Ti) + H_2 \qquad (2)$$

Based on the Equation (1), the TiH_2 basically underwent partial decomposition of H atom at the first stage of the reaction. The temperature at which the H atom began liberated was approximately at 300°C where there was a small endothermic curve with an onset temperature of 350°C as illustrated in Figure 2 (I). From the small endothermic peaks, the large endothermic reaction at temperature 600°C followed as observed in Figure 2 (II). As a matter of fact, the dehydrogenation is a process whereby the TiH_2 absorbed energy to have dissociation of H atom and subsequently produced fresh generated Ti atom [12] that presently accessible for reaction with Nb atoms. The TiH_2 was basically protected the Ti atom from being oxidized because the fresh generated of the Ti was available after 300°C which was the temperature at which partial decomposition occurred, below the temperature. Instead of using Ti which was easily oxidized at low temperature due to high affinity toward oxygen, the TiH_2 could reduce the oxidation process at the initial stage of the heating process. Owing to the interstitial site in its lattice that was already occupied by H atom, this TiH_2 reduced the possibility of dissolution of oxygen atom on the Ti atom respectively [18].

In Figure 2 (II), there was a broad endothermic peak at a temperature around 600°C. According to Liu et al. [8], the peak at around 600°C represented a dehydrogenation process which confirmed that the broad endothermic peak at II was the subsequent thermal event of the dehydrogenation of TiH_2 from the mixture powder sample. Based on the large endothermic peak, the high amount of energy being absorbed by the sample had a phase transition from TiHx to α-Ti as expressed in Equation (2). In other words, the peaks basically corresponded to the phase changes from the face-centered cubic cell (FCC) (TiH_2) with CaF2 crystal structure to hexagonal close packed (HCP) structure [17]. After this phase transition, the α-Ti subsequently was ready for latter diffusion reaction with Nb atom.

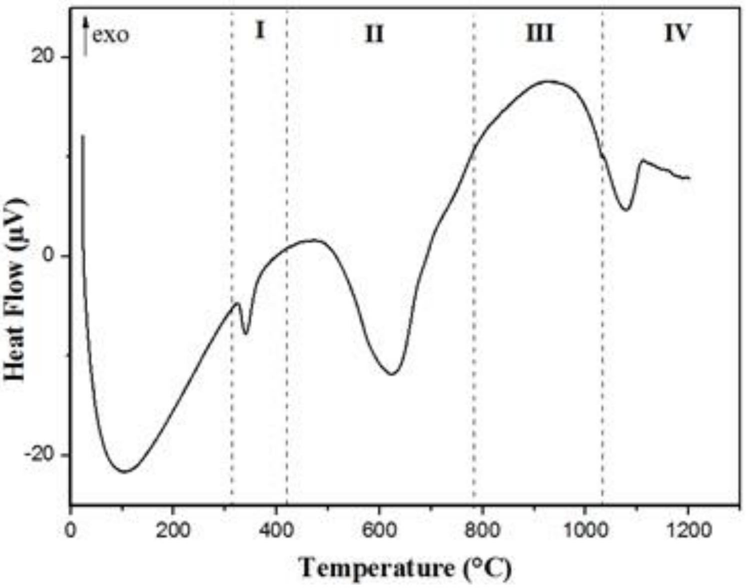

Figure 2: The DTA curve of heat flow varies as a function of temperature for TiNb alloy

Meanwhile, a peak at III as displayed in Figure 2 implied the formation of TiNb alloy. The exothermic reaction in peak III corresponded to the transition phase of the α-Ti hexagonal crystal structure to β-Ti body centered cubic (BCC) structure. The HCP, in fact, had higher slip number rather than BCC structure [19]. Thus, the energy released emphasized that there was a phase transformation from HCP to BCC crystal structure which resulted in the reduction of the slip distance in the particular crystal structure of Ti. On the other hand, the transition of α to β phase transition began nearly at 800˚C (Figure 2). The transition temperature decreased from the 882˚C temperature to 800˚C due to the addition of Nb in Ti alloy in which Nb acted as a beta stabilizer [20]. Figure 2 (IV) showed a small endothermic peak where it might indicate oxidation of Ti at high temperature. These similar findings are reported by Pascu et al. [22] that attributed the endothermic peak to the formation of TiO_2. At 1200°C, it can be seen that the reaction is already in a stable condition [21].

3.2 Dilatometry Analysis

Figure 3 shows the shrinkage curve of Ti-40Nb with respect to temperature. Based on Figure 3, the sintering process of Ti-40Nb alloy consisted of four stages of reaction and this result is consistent with DTA result as illustrated in Figure 2, respectively. The first and second part of the reaction basically indicated dehydrogenation reaction in which this reaction was accompanied by volume expansion. In Figure 3 (I) and (II), the samples expanded a little at a temperature of approximately 300°C and continued until 600°C. This shrinkage curves ideally presented two-step reaction of dehydrogenation process. The large curve corresponded to huge changes in volume due to an increase of intrinsic density of Ti atom itself whereby it was from TiH_2 (3.9 g/ cm^3) to Ti atom (4.5 g/cm^3) respectively. Due to the increase of intrinsic density, supposedly, the sample underwent volume shrinkage as reported in a previous study [15]. However, in this case, the sample expanded. The expansion was derived from the different solubility of the mixed powders which caused swelling and pore formation [22].

The increase of intrinsic density was basically upon the phase change of Ti particle from δ-FCC crystal body structure to α-HCP crystal body structure. The FCC presently has 12 slip system and low slip distance while HCP has 3 to 6 slip system in which it is one-fourth to one-half from FCC slip system with higher slip distance rather than FCC [23]. Thus, the expansion curve resulted from the increase of slip distance of FCC to HCP crystal body structure. The slip distance increases because of heat expansion due to the increase in temperature [24]. Nevertheless, the expansion did not continuously occur. As the heat energy increased and with the presence of Nb as a beta stabiliser, the Ti atom then tended to become β phase resulted in volume shrinkage as illustrated in III. The increase in energy caused the α-Ti in HCP system being packed by Nb atom and other Ti atoms in which at the end, it turned to body cubic crystal (BCC) structure of β-Ti.

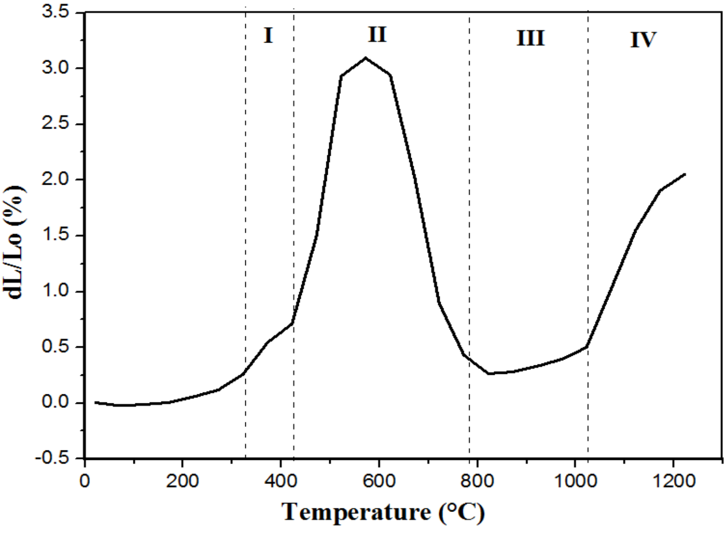

Figure 3: The shrinkage curves of TiNb as a function of temperature

Figure 3 (IV) shows the sample undergoes a slight expand in size. The expansion was probably due to the formation of TiO_2 as mentioned in the DTA analysis. In addition, this expansion was also probably due to the formation of pores. The presence of pores was basically from the Kirkendall effect mechanism that existed because of the difference in the diffusion rate of Ti and Nb as well as rapid exothermic reaction beforehand [25]. The atomic fraction of Nb in this composition of the Ti-40Nb alloy was only 25.73% where it made the Nb to have low density rather than Ti particles. Besides, the Nb had a larger size rather than TiH_2 which affected the diffusion rate. Hence, this led to the Kirkendall pores formation and at the same time caused the diffusion of Ti with Nb which was not too favourable. Thus, the sintering process tended to be dominated by the Ti-Ti diffusion instead of Ti-Nb.

3.3 Phase Identification

Figure 4 shows the XRD pattern for TiH_2 powder, Nb powder, as-mixed powder and as-sintered sample. From the diffraction pattern in (a) and (b) which indicated TiH_2 powder and Nb powder, respectively, the XRD pattern justified the purity of the raw powders in which no impurities exhibited in the diffraction patterns, particularly for both powders. This is the same case for the as-mixed powder by ball milling operation where the intensity peaks at (c) demonstrated the intensity peaks of TiH_2 and Nb powders only.

However, there was a presence of TiO_2 with a space group of P42/mnm, in the sintered sample in small intensity because the sintering process was conducted under argon gas and not in a vacuum condition. This TiO_2 was in the tetragonal crystal structure that formed as a result of stretching the cubic structure. On top of that, there was an exothermic reaction after temperature of around 1000°C. This is consistent with XRD data where there was TiO_2 peaks presence at the as-sintered sample that resulted from the distortion of BCC of β-Ti. The diffraction pattern of TiO_2 in this present work was similar as in a previous study [24].

Besides that, the rich in β phase after sintered at 1200°C was due to diffusion of Nb in Ti lattice progressively. It can be illustrated by the XRD pattern of as-sintered sample where the intensity of β-Ti (space group of Im3m) peaks overlapped with Nb diffraction peaks. In another perspective, it can be concluded that this Nb particle did not completely diffuse in Ti lattice. These data supported the statement that the diffusion in TiNb was being dominated by the diffusion of Ti-Ti instead of Ti-Nb reaction and this was also in accordance to previous research [26].

In respect to the presence of Nb particles that did not completely diffuse in Ti matrix lattice, this Nb also acted as a diffusion barrier as it did not permit the Ti-Ti diffusion. The large size of Nb particles inhibited the diffusion of Ti-Ti particles because Nb did not diffuse completely. This is probably one of the reasons of the minimal densification and shrinkage of the sintered sample. This assumption was in accordance to a study by Zhao et al. [26]. Furthermore, the TiO_2 present was beneficial in promoting good osseointegration and helped in preventing the dissolution of metallic ions into the surrounding cell tissue. Besides, this Ti oxide influenced the mechanical interlocking between the implant and the bone. On the other hand, the TiH_2 had completely undergone dehydrogenation process where there were no traces of TiH_2 in the as-sintered sample. Basically, the diffraction patterns for β-Ti, α-Ti, and Nb were similar as in Zhao et al.'s study [26].

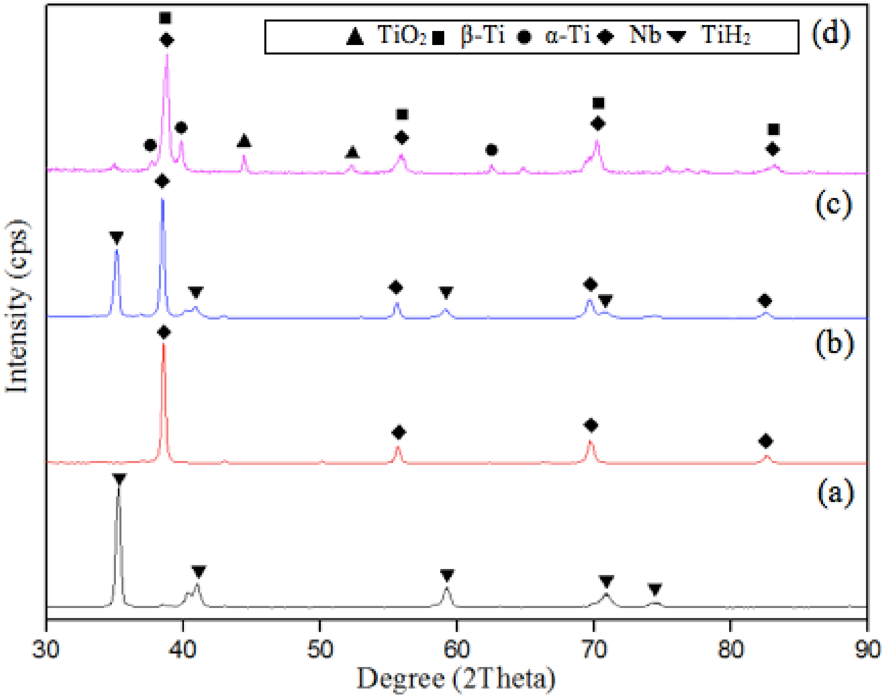

Figure 4: XRD patterns of: (a) TiH_2 powder, (b) Nb powder, (c) As-mixed powder of TiH_2 and Nb mixture and (d) Sintered sample of Ti-40Nb alloy

4.0 CONCLUSION

Based on the thermal analysis result, it can be concluded that the TiH2 undergoes two steps of dehydrogenation process which produces fresh generated Ti atom. After temperature 600°C, this Ti atom is basically ready for the formation with Nb atom resulted in the formation of TiNb alloy for implant application. On the other hand, the other steps represent diffusion process of Ti and Nb alloy. The presence of rich β phase above 1000°C would provide promising excellent mechanical properties that are suitable for implant material. The sintering process is dominated by Ti-Ti diffusion instead of Ti-Nb due to low density and large size of Nb atom. The difference in diffusion rate of Ti and Nb causes Kirkendall effect that leads to the formation of pores. Future study should be carried out in order to attain new implant material with low-cost processing route with promising mechanical properties.

ACKNOWLEDGEMENT

The present work is financially supported by the Ministry of Higher Education (MOHE) under the framework of Research Acculturation Grant Scheme (RAGS) (project code: RAGS/1/2014/TK04/UITM/4). Appreciation and gratitude are also extended to the Research Management Institute of UiTM and Centre for Advanced Material Research (CAMAR), UiTM for facilitating this project.

REFERENCES

[1] M. H. Ismail, "Porous NiTi alloy by metal injection moulding (MIM) using partly water soluble binder system," Ph.D. thesis, Department of Materials Science and Engineering, The University of Sheffield, United Kingdom, 2012.

[2] M.-K. Han, J.-Y. Kim, M.-J. Hwang, H.-J. Song and Y.-J. Park, "Effect of Nb on the microstructure, mechanical properties, corrosion behavior, and cytotoxicity of Ti-Nb Alloys", *Materials,* vol. 8, no. 9, pp. 5986–6003, 2015.

[3] M. Geetha, A. K. Singh, R. Asokamani and A. K. Gogia, "Ti based biomaterials, the ultimate choice for orthopaedic implants – A review", *Progress in Material Sciences*, vol. 54, no. 3, pp. 397–425, 2009.

[4] M. H. Ismail, R. Goodall, H. A. Davies and I. Todd, "Formation of microporous NiTi by transient liquid phase sintering of elemental powders", *Material Sciences and Engineering C*, vol. 32, no. 6, pp. 1480–1485, 2012.

[5] K. Zhuravleva, A. Chivu, A. Teresiak, S. Scudino, M. Calin, L. Schultz, J. Eckert and A. Gebert, "Porous low modulus Ti40Nb compacts with electrodeposited hydroxyapatite coating for biomedical applications", *Material Sciences and Engineering C*, vol. 33, no. 4, pp. 2280–2287, 2013.

[6] G. Chen, P. Cao and N. Edmonds, "Porous NiTi alloys produced by press-and-sinter from Ni/Ti and Ni/TiH_2 mixtures", *Materials Science & Engineering: A*, vol. 582, pp. 117–125, 2013.

[7] J. Davidson and P. Kovacs, "Biocompatible low modulus titanium alloy for medical implants," US Patent US5169597A, 1992.

[8] Y. Liu, L. F. Chen, H. P. Tang, C. T. Liu, B. Liu and B. Y. Huang, "Design of powder metallurgy titanium alloys and composites", *Material Sciences and Engineering A*, vol. 418, no. 1-2, pp. 25–35, 2006.

[9] I. A. Mwamba and L. H. Chown, "The use of titanium hydride in blending and mechanical alloying of Ti-Al alloys", *Journal of the South African Institute of Mining and Metallurgy*, vol. 111, no. 3, pp. 159–165, 2011.

[10] O. M. Ivasishin and V. Moxson, "Low-cost titanium hydride powder metallurgy", *Titanium Powder Metallurgy: Science, Technology and Applications*, pp. 117–148, 2015.

[11] B. Sharma, S. K. Vajpai and K. Ameyama, "Microstructure and properties of beta Ti-Nb alloy prepared by powder metallurgy route using titanium hydride powder", *Journal of Alloys and Compounds.*, vol. 656, pp. 978–986, 2015.

[12] H. H. Mohd Zaki and J. Abdullah, "Comparison studies on solid state diffusion of Ni–Ti and Ni–TiH_2 under CaH_2 reducing environment", *Material Letters*, vol. 121, pp. 36–39, 2014.

[13] S. M. Hosnie, M. H. Ismail, M. Yahaya, N. A. Haris and I. Todd, "Fabrication of porous β-Type Ti-40Nb alloys incorporated with TiH_2 via powder metallurgy processing route under reducing environment", *Journal of Mechanical Engineering*, vol. 2, pp. 99-112, 2017.

[14] Y.-H. Hon, J.-Y. Wang and Y.-N. Pan, "Composition/Phase structure and properties of Titanium-Niobium alloys", *Materials Transactions*, vol. 44, no. 11, pp. 2384–2390, 2003.

[15] H.T. Wang, M. Lefler, Z. Z. Fang, T. Lei, S. Fang, J. Zhang and Q. Zhao, "Titanium and titanium alloy via sintering of TiH_2", *Key Engineering Materials*, vol. 436, pp. 157–163, 2010.

[16] V. Bhosle, E. . Baburaj, M. Miranova and K. Salama, "Dehydrogenation of TiH_2", *Material Sciences and Engineering A*, vol. 356, no. 1-2, pp. 190–199, 2003.

[17] D. Mandrino, I. Paulin and S. D. Škapin, "Scanning electron microscopy, X-ray diffraction and thermal analysis study of the TiH_2 foaming agent", *Materials Characterization*, vol. 72, pp. 87–93, 2012.

[18] H. Wang, Z. Z. Fang and P. Sun, "A critical review of mechanical properties of powder metallurgy titanium", *International Journal of Powder Metallurgy*, vol. 46, no. 5, pp. 45–57, 2010.

[19] W. Ahmed and M. J. Jackson, *Surgical Tools and Medical Devices.* Cham: Springer International Publishing, 2007.

[20] V. A. R. Henriques, E. T. Galvani, S. L. G. Petroni, M. S. M. Paula and T. G. Lemos, "Production of Ti-13Nb-13Zr alloy for surgical implants by powder metallurgy", *Journal of Material Sciences*, vol. 45, no. 21, pp. 5844–5850, 2010.

[21] C.I. Pascu, O. Gingu, P. Rotaru, I. Vida-Simiti, A. Harabor and N. Lupu, "Bulk titanium for structural and biomedical applications obtaining by spark plasma sintering (SPS) from titanium hydride powder", *Journal of Thermal Analysis and Calorimetry*, vol. 113, no. 2, pp. 103–105, 2013.

[22] R. M. German, *Sintering Theory and Practice.* Toronto: John Wiley & Sons, 1996.

[23] F.C. Campbell, *Manufacturing Technology for Aerospace Structural Materials.* Netherlands: Elsevier Science, 2006.

[24] H. Liu, P. He, J. C. Feng and J. Cao, "Kinetic study on nonisothermal dehydrogenation of TiH_2 powders", *International Journal of Hydrogen Energy*, vol. 34, no. 7, pp. 3018–3025, 2009.

[25] K. Mallick, *Bone Substitute Biomaterials.* Netherlands: Elsevier Science, 2014.

[26] D. Zhao, K. Chang, T. Ebel, H. Nie, R. Willumeit and F. Pyczak, "Sintering behavior and mechanical properties of a metal injection molded Ti–Nb binary alloy as biomaterial", *Journal of Alloys and Compounds*, vol. 640, pp. 393–400, 2015.